Multiscale Transform and Shrinkage Thresholding Techniques for Medical Image Denoising – Performance Evaluation

S. Shajun Nisha[1], *S. P. Raja*[2]

[1]*PG and Research Department of Computer Science, Sadakathullah Appa College, Tirunelveli, Tamil Nadu, India*
[2]*Department of Computer Science and Engineering, Vel Tech Rangarajan Dr. Sagunthala R&D Institute of Science and Technology, Avadi, Chennai, Tamil Nadu, India*
E-mails: shajunnisha_s@yahoo.com   avemariaraja@gmail.com

Abstract: *Due to sparsity and multiresolution properties, Mutiscale transforms are gaining popularity in the field of medical image denoising. This paper empirically evaluates different Mutiscale transform approaches such as Wavelet, Bandelet, Ridgelet, Contourlet, and Curvelet for image denoising. The image to be denoised first undergoes decomposition and then the thresholding is applied to its coefficients. This paper also deals with basic shrinkage thresholding techniques such Visushrink, Sureshrink, Neighshrink, Bayeshrink, Normalshrink and Neighsureshrink to determine the best one for image denoising. Experimental results on several test images were taken on Magnetic Resonance Imaging (MRI), X-RAY and Computed Tomography (CT). Qualitative performance metrics like Peak Signal to Noise Ratio (PSNR), Weighted Signal to Noise Ratio (WSNR), Structural Similarity Index (SSIM), and Correlation Coefficient (CC) were computed. The results shows that Contourlet based Medical image denoising methods are achieving significant improvement in association with Neighsureshrink thresholding technique.*

Keywords: *Medical Image Denoising, Multiscale Transforms, Shrinkage Thresholding.*

1. Introduction

Medical imaging has become new research focus area and is playing a significant role in diagnosing diseases. There are many imaging modalities for different applications. All these modalities will introduce some amount of noise like Gaussian, Speckle, Poisson, etc., and artifacts during acquisition or transmission. Suppressing such noise from medical image is still a challenging problem for the medical researchers and practitioners.

1.1. Related work

Image denoising [41-43] is the process of restoration where the attempts are made to recover an image which is been corrupted by some noise. The presence of noise not only produces undesirable visual quality but also lowers the visibility of low contrast objects. Initial methods proposed for image denoising were based on statistical filter [1, 2], but the problems associated with spatial filter during denoising process are that high pass filters amplify noisy background and low pass filter makes the edges blur. When denoising algorithms are employed, they often add some artifacts like blur, staircase effect and many others. To overcome these limitations, multi scale domain operations with certain thresholding techniques in transformation domain is employed. In this paper transforms such as Wavelet, Ridgelet, Curvelet, Contourlet and Bandelet are considered.

Mallat [3] has given multiresolution theory of wavelets. Wavelets have various advantages like no redundancy and efficient implementation. The initial work on wavelet based denoising using thresholding was done by Donoho and Johnstone [4]. By using simple algorithms based on convolution wavelets are easily implementable. The other forms of discrete wavelet transform are Undecimated wavelet transform [5], Dual tree complex wavelet transforms [6] and Double density dual tree complex wavelet transforms [7]. In 1999, Candès and Donoho [8] proposed an anisotropic geometric wavelet transform named Ridgelet. Ridgelet was used for denoising by Chen and Kégl [9]. Bayesshrink Ridgelet denoising technique is proposed and it obtains superior PSNR values when compared to the Visushrink Ridgelet denoising. Straight-line singularities are optimally represented by the Ridgelet transform. To analyse local line or curve singularities, the Ridgelet transform is applied to the partitioned sub images. In 2000, this block Ridgelet based transform called Curvelet transform was proposed by Candès and Donoho [35]. The Curvelet is used for image denoising in papers [11-13]. Starck, Candès and Donoho [14] applied the Curvelet and Ridgelet transforms to the denoising of some standard images embedded in white noise and it is reported that simple thresholding of the Curvelet coefficients is very competitive with other techniques based on wavelet transform. The Curvelet based reconstructions provide higher quality, visually sharper images, and faint linear and curvilinear features.

Geometrical structures are important when medical images are processed. There are several transforms that tackle the problem of image geometry such as the Contourlet or Bandlet transform. The second generation Bandlet transform is a 2D wavelet transform followed by a Bandletization. The Bandlet is an orthogonal, multiscale transform able to preserve the geometric content of images and surfaces [15]. A comparison of the Bandlet, Wavelet and Contourlet Transforms for image denoising can be found [16]. In paper [17], a novel image denoising method is proposed based on the symmetric normal inverse Gaussian model and the non-subsampled Contourlet transform. Eslami and Radha [18] constructed semi translation invariant Contourlet transform to achieve an efficient image denoising approach. A despeckling algorithm is proposed [19] based on non-subsampled Contourlet transform for the speckle noise reduction in the CT medical image

processing. The algorithm aims to denoise the speckle noise in ultrasound image using adaptive binary morphological operations, in order to preserve edge, contours and textures. In paper [20], a new algorithm is proposed using Contourlet which is combined with the thresholding Technique for magnetic resonance imaging reconstruction. A two stage multimodal fusion framework is presented [21] using the cascaded combination of stationary wavelet transform and non sub-sampled Contourlet transform. The merit of using this approach is to improve the shift variance, directionality and phase information in the finally fused image. Wavelet, Bandlet and Ridgelet presented a comparative analysis of JPEG, and it is applied to images of chromosomes.

Thresholding removes certain coefficient, which falls below a certain value. The coefficients retrieved undergo further processing where denoising method is applied to them based on selected threshold method. The retrieval of coefficients and application of threshold at each level helps identify noise clearly and effectively. Choosing a threshold is main concerned issue. Careful balance of threshold cut-off is an important aspect, as one cannot discard too many coefficients leading to smoothing and neither very few coefficients leading to under smoothed estimate [23]. Researchers published different ways to compute the parameters for the thresholding of wavelet coefficients. In the recent years there has been a fair amount of research on wavelet thresholding and threshold selection for image de-noising [24, 25], because wavelet provides an appropriate basis for separating noisy signal from the image signal. The motivation is that as the wavelet transform is good at energy compaction, the small coefficient is more likely due to noise and large coefficient due to important signal features. Data adaptive thresholds [26] were introduced to achieve optimum value of threshold. Translation invariant methods based on thresholding of an undecimated wavelet transform were presented [27]. These thresholding techniques were applied to the non-orthogonal wavelet coefficients to reduce artifacts.

Application of universal threshold in wavelet transform for denoising an image is Visushrink [27], which is automatic and fast thresholding method. It is quite easy where a simple threshold function is applied to obtained coefficients of the image. Sureshrink provides more detailed image, hence giving better results than Visushrink [28]. This method is best suited for images inculcated with Gaussian noise [29]. The drawback of Sureshrink method is that consideration of sparsity where local neighborhood of each coefficient is neglected resulting in biased estimator hence removing many terms from derived coefficients. To overcome this and increase precision of estimation, NeighBlock approach came in the picture that utilizes information of neighboring pixels. Consideration of neighboring pixels helps in deciding the threshold value. This method is best in case of Doppler signal. In this method, min-max or principle of minimum value and maximum value is considered. A fixed threshold is used for estimating mean square error of coefficients. Heursure is a method that is made by combining SURE and global thresholding method. The drawback of SURE method when applied to signal-to noise ratio being very small resulting in more noises is overcome by heursure method that accounts for a fixed

threshold selection by global thresholding method. Recently many medical image denoising frameworks are proposed [30-33] based on wavelet transform.

1.2. Motivation and Justification of the proposed work

In this paper a method for denoising medical images is proposed based on the combination of Multiscale transforms. The main advantage of the Multiscale transforms is that it can describe local features either spatially or spectrally, which makes it to filter out most of noise while at the same time preserving the edges and fine details. On applying Mutiscale transforms to decompose an image it yields a set of detail subband having wavelet coefficients and an approximation subband having scaling coefficients. Motivated by these facts, in this paper Multiscale transforms based technique is employed.

Energy becomes more concentrated into fewer coefficients in the transform domain, which is an important principle that enables the separation of signal from noise. Transform coefficients are typically estimated by wavelet shrinkage which retain the coefficients that are more likely to represent the actual signal in the image and heavily suppress those coefficients that represent noise. In this scheme, coefficients above the threshold are shrunk by the absolute value of the threshold itself for medical noise removal. Justified by these facts, in this paper Multiscale transforms based technique are combined with shrinkage thresholding techniques for medical image denoising.
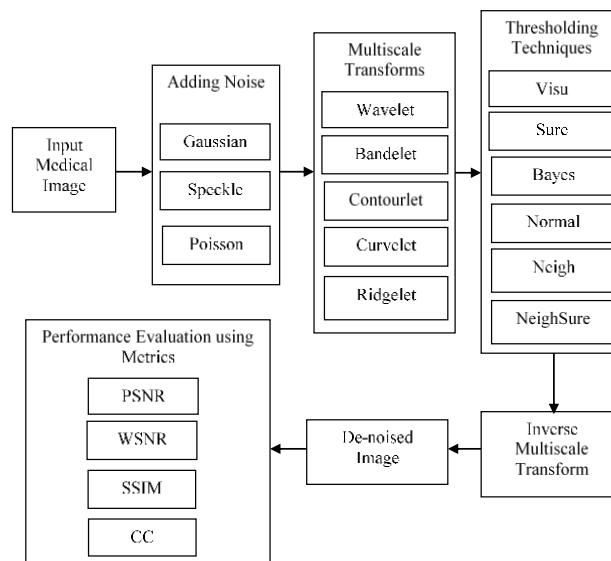
Fig. 1. Outline of the proposed approach

1.3. Contributions

The main novelties of this work are as follows.

1. Previous studies showed that Medical image denoising is done with wavelet transform. In this work, multiscale transforms (wavelet, curvelet, contourlet, ridgelet and bandlet) are taken into consideration for medical image denoising.

133

2. Literature study shows that most of the previous works dealt with any particular noise. In this work, Gaussian, speckle and Poisson noises are considered.

3. Considering the Image Modality previous works dealt with any one type of image modalities. In this work, MRI, CT and X-Ray are considered.

4. Finally, past works were done by taking one particular thresholding technique. In this work, six types of thresholding techniques are considered.

1.4. Outline of the proposed work

The entire process is of denoising shown is Fig. 1. Noise added image is decomposed using any one of multiscale transform which yields coefficients. The values of such coefficients differ according to the signal or noise. Hence, thresholding techniques are applied to cut off noisy coefficients. The remaining coefficients can be inverse transformed to get the denoised image. The Quality of denoised image can be compared with original image using performance metrics.

2. Mathematical model of noises

Speckle noise is also known as texture in medical literatures. Generalized model of the speckle is represented in the equation

(1) $$g(n, m) = f(n, m)*u(n, m) + \xi(n, m).$$

Here, $g(n, m)$ is the observed image, $f(n, m)$ is the input image, $u(n, m)$ is the multiplicative component, $\xi(n, m)$ is the additive component, and n and m are the axial and lateral indices.

Gaussian noise is evenly distributed over the signal. The distribution function $f(g)$ is given by

(2) $$f(g) = \frac{1}{\sqrt{2\pi\sigma^2}} e^{-(g-m)^2/2\sigma^2},$$

where g represents the grey level, m is the mean or average of the function and σ is the standard deviation of the noise. Poisson noise follows a Poisson distribution, which is usually not very different from Gaussian. The noise in X-ray imaging and Nuclear Imaging (PET, SPECT) is modelled with Poisson noise. The probability of Poisson density $P(f(x))$ is given in the equation

(3) $$P(f(x) = k) = \frac{\lambda^k e^{-\lambda}}{k!}.$$

Here λ is the shape parameter and $k = 0, 1, 2....$

3. Multiscale transforms

The Discrete Wavelet Transform (DWT) is obtained by a successive low pass filter and a high pass filter. Fig. 2 shows the steps to obtain the DWT coefficients. In the decomposition stage, the input image is passed to the low pass filter (y_δ) and a high pass filter (y_γ) to obtain the coarse approximations. Also it creates the detailed information about the given input image. The down sampling is referred as ↓. The up sampling is referred as ↑. This process is repeated to all the rows to obtain the wavelet coefficients.
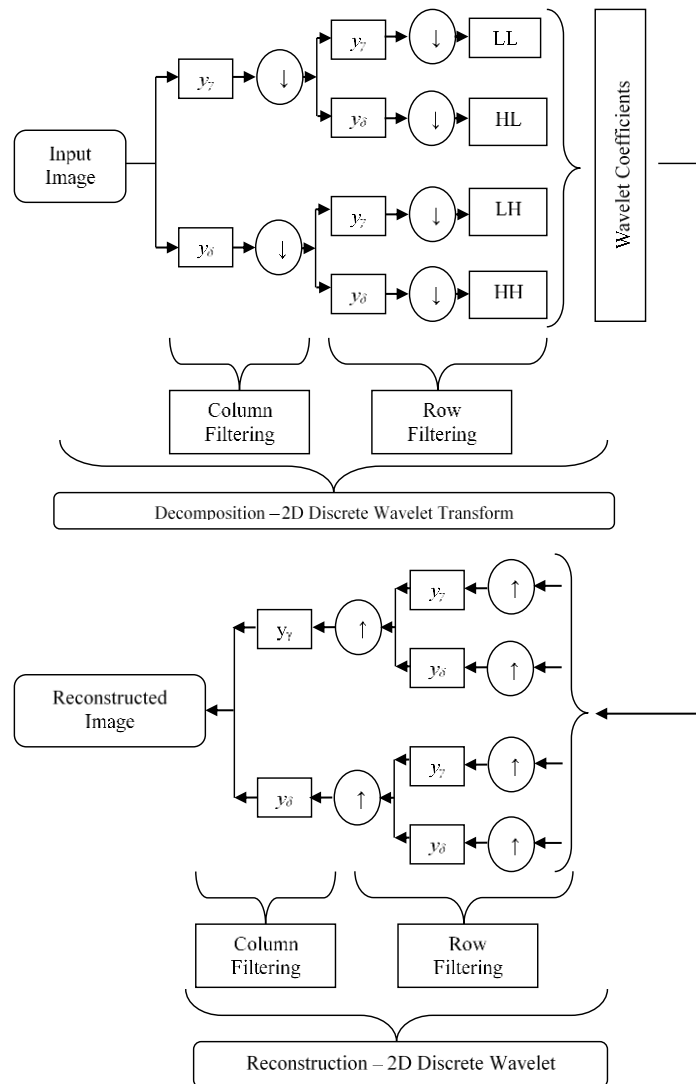
Fig. 2. Wavelet decomposition

After applying DWT (one level) to an input image, it is decomposed into four subbands. They are Low Low (LL), High Low (HL), Low High (LH) and High High (HH) subbands. The LL band has significant information and all the other bands are having less significant information. Ridgelet transform [34] is done in two steps: a calculation of discrete Radon transform and an application of a wavelet transform. The main application of Ridgelet transform is to represent objects with line singularities. Curvelet transform [35] is the most suitable for objects with curves. For Curvelet Transform, initially the image is partitioned into sub-images and then the Ridgelet transform is applied as shown in Fig. 3. This blocking Ridgelet based transform was named as Curvelet Transform, which is also called as First Generation

135

Curvelet transform. Later Second Generation Curvelet Transform was proposed and it is used in many applications like image denoising, image enhancement and compressed sensing.
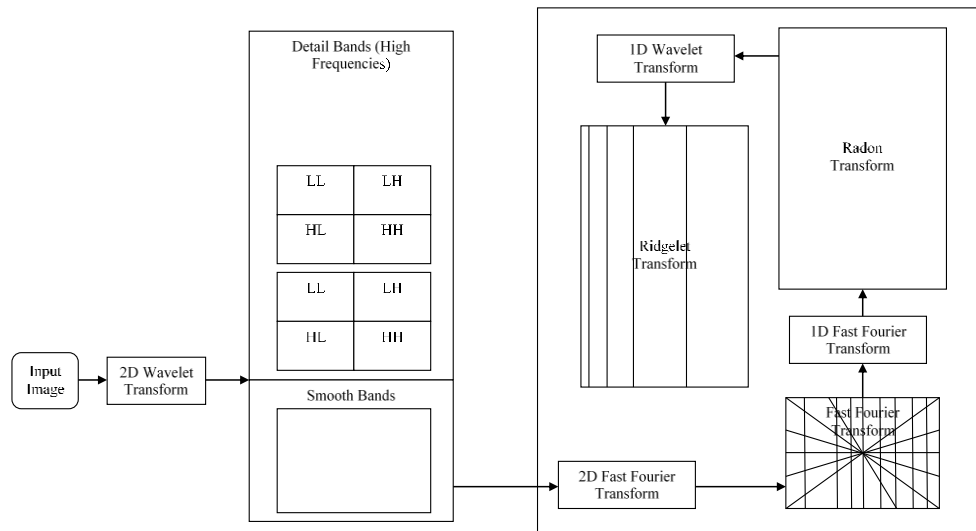

Fig. 3. Curvelet transform [35]

The contourlet transform [36] is shown in Fig. 4. Laplacian Pyramid (LP) was used for the subband decomposition and Directional Filter Banks (DFB) was used for the directional transform. In the Laplacian pyramid, the spectrum of the input image will be divided into the lowpass subband and the highpass subband. Then, the lowpass subband will be downsampled by two both in the horizontal and vertical direction and passed onto the next stage. The highpass subband will be further separated into several directions by the directional filter banks. The contourlet transform has used in many applications like image enhancement, radar despeckling and texture classification.

The First generation Bandlet transform was developed by L e P e n n e c and M a l l a t [37] based on 2D separable Wavelet Transform. In the first generation Bandlet transform, initially the given image is segmented into macro-blocks like a quad-tree structure. The geometric flow of each macro-block is determined. The wavelet functions are warped to adapt to the flow line of each macro-block. Then Bandletization is performed to solve vanish moment problem of the scaling function. Finally, perform separable 2D wavelet transform. It is shown in Fig. 5. The Second Generation Bandlet Transform was proposed by P e y r e and M a l l a t [38] to overcome the demerits of sampling and curving in the first generation.
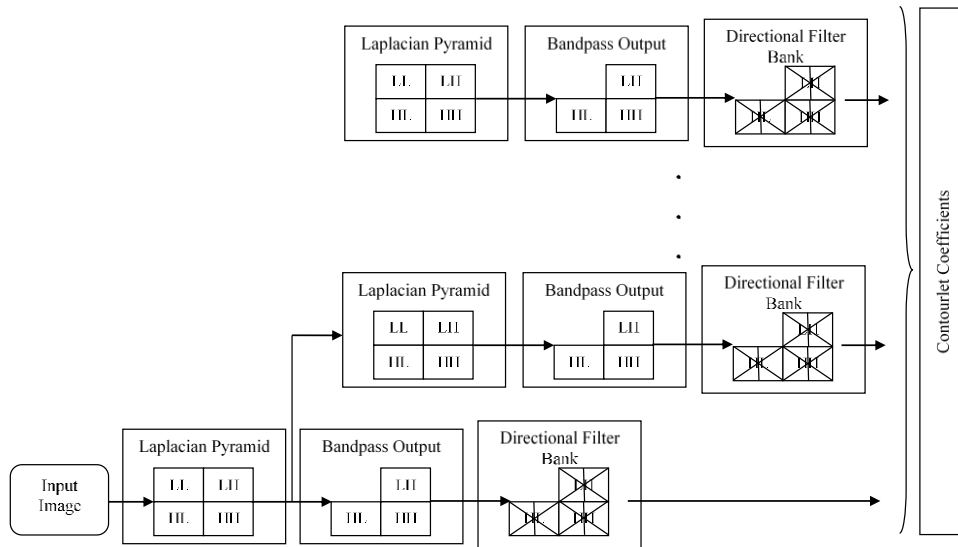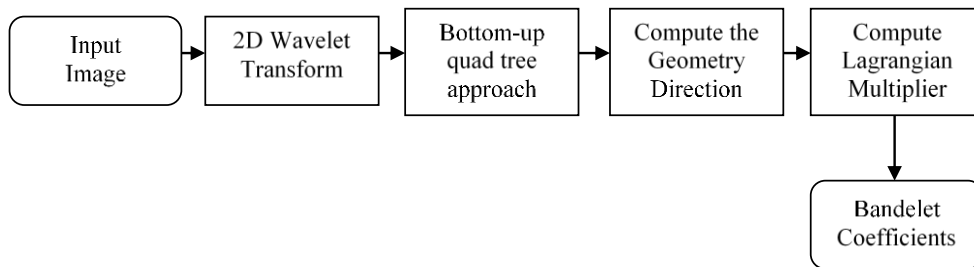
136

Fig. 4. Contourlet transform [36]

Fig. 5. Bandlet transform [38]

The thresholding approaches used in the paper are Visushrink, Sureshrink, Neighshrink, Bayesshrink, Normalshrink and Neighsureshrink. VisuShrink threshold is computed by applying the Universal threshold and it follows the hard thresholding rule. The Sureshrink threshold is a combination of Universal threshold and SURE threshold. The goal of Sureshrink is to minimize the MSE. Bayesshrink is used to minimize the Bayesian risk, and hence its name, Bayesshrink. Normalshrink is a threshold value which is adaptive to different sub band characteristics. In Neighshrink [39], a square neighboring window centered for each noisy wavelet coefficient to be shrinked will be taken. Neighsureshrink [40] is an improvement over Neighshrink, which has disadvantage of using a non-optimal universal threshold value and the same neighboring window size in all wavelet sub bands. Neighsureshrink can determine an optimal threshold and neighboring window size for every sub band by the Stein's Unbiased Risk Estimate (SURE).

4. Experiments and results

4.1. Experiments and experimental data

MRI, X-RAY and CT images are taken for experimental purpose for denoising. We considered Gaussian, Speckle and Poisson noises only for this study. Fig. 6 shows the original image and noised images.
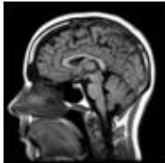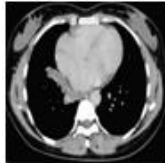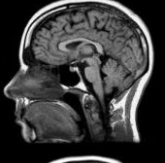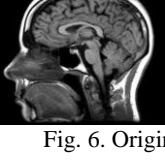
Image	MRI	CT	X-RAY
Original Image			
Gaussian Noised Image			
Speckle Noised Image			
Poisson Noised Image			

Fig. 6. Original and noisy images

4.2. Experimental Output

Experiments were conducted on two aspects. The first one is image sources versus the noises. The second one is Multiscale transform versus shrinkage thresholding techniques. We conducted three experiments, one for each image source. We considered mainly PSNR metric to determine the best combination. As it is expected that the performance will vary according to the level of decomposition and the amount of noise present in the image, two more experiments were conducted, keeping the two best performing Multiscale transforms and the best two thresholding techniques. From the experimental results it is observed that the best performing multiscale transforms are Wavelet and Contourlet. Hence, Fig. 7 shows the output of denoised images only for these two transforms at level 2 and level 3 decomposition. It is also evident that the performance of the Contourlet is slightly better than Wavelet. Hence, Fig. 8 shows the denoised images output at different noise variance of Gaussian, Speckle and Poisson noises.

Noise	Transform	Level	MRI	CT	X-RAY
Gaussian	Wavelet	2			
		3			
	Contourlet	2			
		3			
Speckle	Wavelet	2			
		3			
	Contourlet	2			
		3			
Poisson	Wavelet	2			
		3			
	Contourlet	2			
		3			
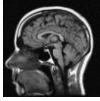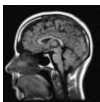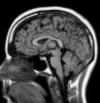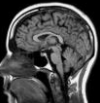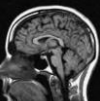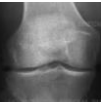
Fig. 7. Denoised images for Wavelet and Contourlet

Noise	Variance	MRI		CT		X-RAY	
		Noisy Image	Denoised Image	Noisy Image	Denoised Image	Noisy Image	Denoised Image
Gaussian	0.2						
	0.4						
	0.6						
Speckle	0.2						
	0.4						
	0.6						
Poisson	0.2						
	0.4						
	0.6						
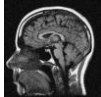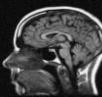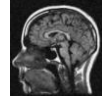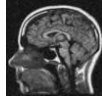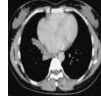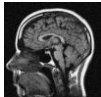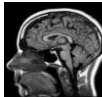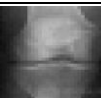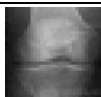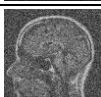
Fig. 8. Denoised images for different Noise Variance

5. Performance evaluation

The purpose of the experiments is twofold. The first one is to identify the best performing multiscale transform. The second one is to find the best performing shrinkage thresholding technique. This is to be tested against MRI, CT and X-RAY imaging modalities and as well against Gaussian, speckle and Poisson noises using PSNR metric. The first experiment is conducted to identify the best suitable bases for the wavelet. Biorthogonal, Reverse Biorthogonal, Daubechies, Coiflets and Symlets were considered and results are shown in Table 1. The SSIM index can be viewed as a quality measure of one of the images being compared provided the other image is regarded as of perfect quality. SSIM is ranging from 0 (low qulity) to 1 (high quality) which has no units.

140

Table 1. Performance of Wavelet bases for Denoising

Metric	Wavelet type	Gaussian	Poisson	Speckle
PSNR (in dB)	Biorthogonal	**21.183**	**18.09**	29.851
	Reverse biorthogonal	21.166	18.065	29.867
	Daubechies	21.140	18.088	29.822
	Coiflets	21.158	18.087	29.864
	Symlets	21.177	18.113	**29.875**
WSNR (in dB)	Biorthogonal	**25.414**	22.143	33.823
	Reverse biorthogonal	25.405	22.111	33.838
	Daubechies	25.374	22.143	33.785
	Coiflets	25.395	22.134	33.851
	Symlets	25.419	**22.154**	**33.871**
SSIM	Biorthogonal	0.821	**0.782**	**0.891**
	Reverse biorthogonal	0.815	0.765	0.872
	Daubechies	0.817	0.754	0.887
	Coiflets	**0.829**	0.763	0.855
	Symlets	0.815	0.759	0.866

In the second experiment performance of different multiscale transforms were studied using PSNR in association with Visushrink, Sureshrink, Neighshrink, Bayesshrink, Normalshrink and Neighsureshrink thresholding techniques for denoising MRI images. Results are shown in Table 2. This setup is repeated with CT and X-RAY images and is presented in Table 3 and Table 4 respectively. In order to study the effect of level of decomposition of the transform, another experiment is conducted for the best performing top most transforms and is presented in Table 5. The amount of noise removed depends on the amount of noise added or acquired in the image. Hence, noises were added at different variance levels and their performance is shown in Table 6. From Table 1, it is observed that Symlet bases perform well in Wavelet category. Hence, this wavelet is compared with all other multiscale transforms on remaining experiments. From the experimental results from Table 2, for MRI images, it is evident that Contourlet is the best suited for removing Gaussian noises. It is also seen that, Wavelet and Contourlet perform equally for removing Speckle and Poisson noises. From the same table, it is also observed that the neighsureshrink coefficient shrinkage thresholding techniques perform better than the other techniques. For denoising CT images, Table 3 reveals Contourlet is better choice. For X-Ray images, Table 4 concludes that speckle and Poisson noises are better removed using wavelet and Contourlet. It is also observed that Contourlet removes Gaussian noise well. It is expected that when the level of decomposition varies, the performance of denoising may deteriorate. Since Contourlet and wavelet performs superior in denoising, we have taken these two techniques for level decomposition study. From the output in Table 5, it is observed that level 3 decomposition is sufficient to yield significant improvement. One can easily expect that, as the amount of noise increases in the image, the denoising performance will decrease. It is evident from the Table 6, noise removal techniques are performing well even when 40% of the images are corrupted.

Table 2. Performance of the Coefficients Shrinkage Thresholding techniques for MRI images

Noises	Shrinkage Thresholding technique						
	Multi resoultion	Visu shrink	Sure shrink	Bayes shrink	Normal shrink	Neigh shrink	Neighsure shrink
Gaussian	Wavelet	25.1202	25.4954	25.2211	25.5147	25.5507	25.6687
	Bandlet	20.3756	20.3435	19.6772	20.0012	20.119	20.5089
	Ridglet	24.3242	24.6965	24.4699	24.4894	24.4914	24.7703
	Curvelet	23.1223	23.2089	23.2808	23.5652	23.6938	23.5975
	Contourlet	**26.1126**	**26.0251**	**26.065**	**26.6135**	**26.1746**	**26.6996**
Speckle	Wavelet	**30.4499**	30.4913	**30.6097**	**30.6865**	**30.8715**	**30.9687**
	Bandlet	28.6624	28.4714	28.6126	28.8162	29.868	29.5089
	Ridglet	29.4367	28.1857	28.36	29.5309	28.5085	29.5703
	Curvelet	28.2366	28.7731	29.488	28.4624	29.465	28.6975
	Contourlet	30.2401	**30.5426**	30.4263	30.4919	30.4715	30.7949
Poisson	Wavelet	32.6703	33.7739	33.6828	**34.2781**	33.8331	34.7116
	Bandlet	**33.9117**	33.1381	33.6382	33.8742	**33.9858**	**34.8907**
	Ridglet	30.8126	30.7255	31.4377	31.4925	31.4935	31.7872
	Curvelet	29.9334	30.7738	30.5505	30.5367	31.589	31.5158
	Contourlet	32.1983	**33.9028**	**33.7073**	33.701	33.6821	34.5174

Table 3. Performance of Coefficients Shrinkage Thresholding techniques for CT images

Noises	Shrinkage Thresholding technique						
	Multi Resoultion	Visu shrink	Sure shrink	Bayes shrink	Normal shrinkl	Neigh shrink	Neighsure shrink
Gaussian	Wavelet	25.07	25.072	26.144	**26.1952**	26.1687	26.3687
	Bandlet	23.27	23.272	23.5144	23.3952	23.3687	23.3687
	Ridglet	23.5342	22.7705	21.2085	21.1509	21.1912	24.1912
	Curvelet	23.8542	23.0905	21.5285	21.4709	21.5112	24.5112
	Contourlet	**25.7537**	**26.3114**	**26.3161**	26.0546	**26.7116**	**26.7116**
Speckle	Wavelet	27.0786	27.3768	**27.5553**	**27.3039**	27.3089	27.7089
	Bandlet	26.2786	26.29768	26.7553	26.5039	26.5089	26.355
	Ridglet	**28.1192**	25.7686	25.1874	26.0745	26.1648	26.1648
	Curvelet	23.4392	23.0886	21.5074	21.4945	21.4848	23.4848
	Contourlet	27.9056	**27.9804**	27.2454	27.0667	**27.8907**	**27.9907**
Poisson	Wavelet	32.0558	32.141	32.6001	32.14471	32.3703	32.5703
	Bandlet	30.2558	30.341	30.8001	31.06471	31.5703	31.6703
	Ridglet	28.0515	29.7622	29.2148	30.1722	30.1736	30.1736
	Curvelet	30.3715	31.0822	31.4348	31.4922	30.4936	30.5493
	Contourlet	32.2611	32.6231	32.128	32.6929	32.7872	32.9787

Table 4. Performance of Coefficients Shrinkage Thresholding techniques for X-Ray images

Noises	Multi resoultion	Visu shrink	Sure shrink	Bayes shrink	Normal shrink	Neigh shrink	Neighsure shrink
				Shrinkage Thresholding technique			
Gaussian	Wavelet	26.1559	26.0957	26.25197	26.1177	26.3948	26.5292
	Bandlet	23.5169	24.1042	23.1456	24.1116	24.1822	24.41102
	Ridglet	22.2134	24.1929	23.7597	22.2146	24.7861	24.7878
	Curvelet	23.8551	24.0148	25.9313	22.0179	24.9484	25.9431
	Contourlet	**27.8978**	**28.2302**	**28.445**	**28.2412**	**28.618**	**28.7531**
Speckle	Wavelet	**32.4928**	32.048	**32.5445**	32.12	32.9716	33.7381
	Bandelet	30.1471	30.1586	30.2314	30.1561	31.4275	31.6895
	Ridglet	31.9945	31.1716	31.2077	31.1955	31.611	32.997
	Curvelet	31.5069	31.2721	31.713	31.3168	31.8221	32.2046
	Contourlet	32.1715	**33.79612**	32.1243	**32.1251**	**33.501**	**33.8874**
Poisson	Wavelet	36.0176	**36.1957**	36.5461	36.2485	**36.5507**	36.8331
	Bandelet	32.8286	32.1989	32.4618	28.2249	30.119	33.9858
	Ridglet	33.4691	33.0836	33.8073	33.1011	33.4914	33.4935
	Curvelet	34.6795	34.18	34.3498	33.2014	33.6938	33.7589
	Contourlet	**36.7837**	36.1616	**36.9562**	**37.2898**	36.1746	**37.6821**

Table 5. Performance of Wavelet and Contourlet at different decomposition level

Noise types	Multilets	Levels	XRAY		CT SCAN		MRI	
			Neigh shrink	Neighsure Shrink	Neighs hrink	Neighsure shrink	Neigh shrink	Neighsure shrink
Gaussian	Wavelet	1	25.2056	26.7501	25.3144	25.1952	25.1687	25.6187
		2	26.2331	27.7651	26.5553	26.3039	26.3089	27.0893
		3	26.4761	27.794	26.6001	26.6471	**26.3703**	**27.7083**
		4	**26.5202**	**27.8915**	**26.6438**	**26.8441**	26.2975	27.5279
	Contourlet	1	31.2738	31.673	27.4928	27.5461	27.7116	**29.9216**
		2	31.2442	32.0297	28.1471	29.4618	**27.8907**	29.8907
		3	31.4518	32.3853	**28.9945**	**29.8073**	27.7872	29.7872
		4	**31.7283**	**32.4308**	28.5069	29.3498	27.5158	29.5158
Speckle	Wavelet	1	31.5909	32.4444	24.1715	25.9562	32.3114	33.3161
		2	**32.7257**	32.5251	24.4928	**26.5445**	**33.9804**	34.2454
		3	32.6388	**33.8455**	**25.1471**	26.2314	33.6231	34.128
		4	32.4614	32.5649	23.9945	24.2077	34.778	**33.7651**
	Contourlet	1	32.565	33.5234	**29.3948**	**29.9716**	33.1509	**34.1912**
		2	**35.4058**	**36.4058**	29.1822	29.4275	33.1745	34.1648
		3	32.3949	33.8819	28.7861	28.611	33.1722	34.1736
		4	29.2531	29.7383	28.9484	28.8221	**33.1907**	34.1896
Poison	Wavelet	1	27.5343	28.7559	29.618	30.501	28.0957	29.048
		2	27.548	**28.8154**	**33.2928**	**33.7381**	28.1042	**29.1586**
		3	**27.8884**	28.445	33.1102	33.6895	**28.1929**	24.1716
		4	26.98	27.5859	32.7878	32.997	28.0148	24.2721
	Contourlet	1	**30.5507**	**30.5147**	27.7116	28.0546	28.4709	**29.5112**
		2	30.119	30.0012	**27.8907**	28.9667	28.4945	29.4848
		3	29.4914	29.4894	27.7872	**28.9294**	28.4922	29.4936
		4	29.6938	29.5652	27.5158	28.7801	**28.5107**	29.5096

Table 6.   Performance of Denoising at different noise level

Noises	Noise	XRAY					CT SCAN					MRI				
		Noise image PSNR	PSNR	WSNR	SSIM	CC	Noise Image PSNR	PSNR	WSNR	SSIM	CC	Noise image PSNR	PSNR	WSNR	SSIM	CC
Gaussian	0.2	**22.4581**	**23.787**	**25.246**	**0.91**	**0.95**	21.046	**23.314**	**25.195**	**0.95**	**0.95**	**20.110**	**21.064**	**23.4625**	**0.95**	**0.95**
	0.4	21.1109	22.980	24.714	0.88	0.92	**21.553**	22.553	24.303	0.89	0.92	20.0928	20.679	22.1478	0.890	0.92
	0.6	20.5884	21.625	23.818	0.85	0.84	17.209	21.6	23.447	0.87	0.82	19.1102	19.791	22.818	0.89	0.81
	0.8	18.1524	19.749	22.836	0.82	0.66	18.329	19.644	22.414	0.83	0.61	18.7878	18.911	22.545	0.89	0.64
Speckle	0.2	**23.6147**	24.086	25.706	**0.94**	**0.95**	**23.516**	24.172	**25.956**	**0.95**	**0.95**	20.205	21.064	**23.568**	**0.96**	**0.95**
	0.4	22.6249	**24.119**	25.758	0.92	0.92	23.349	**24.493**	24.544	0.92	0.92	**20.7381**	20.791	23.480	0.89	0.92
	0.6	22.0237	24.105	**25.878**	0.92	0.86	22.917	23.147	24.231	0.89	0.87	19.6895	**20.871**	22.845	0.9	0.84
	0.8	22.6058	24.118	25.697	0.91	0.65	22.683	23.995	23.207	0.89	0.64	19.997	19.475	20.5741	0.89	0.64
Poisson	0.2	**19.4175**	**21.760**	**22.431**	**0.90**	**0.95**	**19.906**	**21.618**	**22.501**	**0.94**	**0.95**	18.2046	**21.095**	**24.048**	**0.952**	**0.95**
	0.4	18.6285	19.896	21.289	0.89	0.92	18.709	19.293	21.738	0.91	0.92	**20.8331**	20.104	22.1586	0.92	0.92
	0.6	16.9815	17.691	21.114	0.89	0.88	16.402	17.11	21.689	0.90	0.88	19.9858	19.192	21.1716	0.92	0.85
	0.8	15.3464	16.039	20.264	0.87	0.67	15.293	16.788	20.997	0.88	0.62	18.4935	18.014	20.2721	0.893	0.63

6. Conclusion

Image denoising has been a classical problem in medical image processing. In this study, we have summarized and implemented various effective denoising algorithms based on multiscale transform schemes for the purpose of image denoising and assessed their performances. In this paper, the advantages and applications of popular standard transforms such as wavelet, Bandlet, Ridgelet, Curvelet and Contourlet are realized for image denoising. When different wavelets are iteratively considered for decomposition and reconstruction of the image while denoising, it is found that the Haar base has the best output. On comparing all multiscale transforms, it is observed that Contourlet is outperforming all other techniques for medical image denoising. We have seen that coefficient thresholding is an effective method of denoising noisy signals. Threshold selection is a big challenge for image denoising. The experiments were conducted for the study and understanding of different thresholding techniques which are the most popular. We then investigated many soft thresholding schemes such as Visushrink, Sureshrink, Bayesshrink, Normalshrink, Neighshrinkand Neighsureshrink for denoising images. The performance is statistically validated and compared to determine the advantages and limitations of all type of shrinkage techniques Neighsureshrinkthreshold function is better as compared to other threshold function. From the comparative analysis of all the above described denoising algorithms, it has been observed that combination of Contourlet with Neighsureshrink shrinkage thresholding technique does perform better than the existing techniques.

R e f e r e n c e s

1. B h o n s l e, D., V. C h a n d r a, G. R. S i n h a. Medical Image Denoising Using Bilateral Filter. I. J. Image. – Graphics and Signal Processing, Vol. **4**, 2012, No 6. pp. 36-43. DOI:10.5815/ijigsp.2012.06.06.
2. G o n z a l e z, R. C., R. E. W o o d s. Digital Image Processing. Second Ed. Prentice-Hall, Inc., 2002.

3. M a l l a t, S. G. A Theory for Multiresolution Signal Decomposition: The Wavelet Representation. – IEEE Transaction on Pattern Recognition and Machine Intelligence, Vol. **11**, 1987, No 7. pp. 674-695. DOI:10.1109/34.192463.

4. D o n o h o, D. L., I. M. J o h n s t o n e. Adatpting Tounknow Smoothness via Wavelet Shrinkage. – Journal of the American Statistical Association, Vol. **90**, 1995, No 432. pp. 1200-1224. DOI:10.1.1.161.8697.

5. Z h a n g, M., B. K. G u n t u k. Multiresolution Bilateral Filtering for Image Denoising. – IEEE Transactions on Image Processing, Vol. **17**, 2008, No 12, pp. 2324-2333.

6. C o i f m a n, R., D. D o n o h o. Translation Invariant Denoising. – In: Lecture Notes in Statistics: Wavelets and Statistics. Vol. **1995**. New York, Springer-Verlag. 1995, pp. 125-150.

7. S e l e s n i c k, I. W. The Double Density Dual Tree DWT. – IEEE Transactions on Signal Processing, Vol. **52**, 2004, No 5, pp. 1304-1314.

8. C a n d è s, E. J., D. L. D o n o h o. Curvelets: A Surprisingly Effective Nonadaptive Representation for Objects with Edges in Curve and Surface Fitting. Nashville, TN: Vanderbuilt Univ. Press, 2000.

9. C h e n, G. Y., B. K é g l. Image Denoising with Complex Ridgelets. – Elsevier, Pattern Recognition, Vol. **40**, 2007, No 2, pp. 578-585.

10. N e z a m o d d i n i-K a c h o u i e, N., P. F i e g u t h, E. J e r n i g a n. Bayes Shrink Ridgelets for Image Denoising. – Springer, ICIAR, LNCS 3211, 2004, pp.163-170.

11. P a t i l, A. A., J. S i n g h a i. Image Denoising Using Curvelettransform: An Approach for Edge Preservation. – Journal of Scientific & Industrial Research, Vol. **69**, 2010, No 1, pp. 34-38.

12. B a l a, A. A., C. H a t i, C. H. P u n i t h. Image Denoising Method Using Curvelet Transform and Wiener Filter. – International Journal of Advanced Research in Electrical, Electronics and Instrumentation Engineering. Vol. **3**, 2014, No 1.

13. S t a r c k, J.-L., E. J. C a n d è s, D. L. D o n o h o. The Curvelet Transform for Image Denoising. – IEEE Transactions on Image Processing, Vol. **11**, 2002, No 6, pp. 670-684.

14. S t a r c k, J.-L., E. J. C a n d e s, D. L. D o n o h o. The Curvelet Transform for Image Denoising. – IEEE Transactions on Image Processing, Vol. **11**, 2002, No 6, pp. 670-684.

15. M a l l a t, S., G. P e y r é. A Review of Bandlet Methods for Geometrical Image Representation. – Numerical Algorithms, Vol. **44**, 2007, No 3, pp. 205-234.

16. V i l l e g a s, O. O. V., H. J. O. D o m í n g u e z, V. G. C. S á n c h e z. A Comparison of the Bandelet, Wavelet and Contourlet Transforms for Image Denoising. – In: Proc. of 7th Mexican International Conference on Artificial Intelligence, 2008, pp 207- 212.

17. Z h o u, Y., J. W a n g. Image Denoising Based on the Symmetric Normal Inverse Gaussian Model and Non-Subsampled Contourlet Transform. – IET Image Processing, Vol. **6**, 2013, No 8, pp. 1136-1147.

18. E s l a m i, R., H. R a d h a. Translation Invariant Contourlet Transform and Its Application to Image Denoising. – IEEE Transactions on Image Processing, Vol. **15**, 2006, No 11, pp. 3362-3374.

19. B a b u, J. J. J., G. F. S u d h a. Non-Subsampled Contourlet Transform Based Image Denoising in Ultrasound Thyroid Images Using Adaptive Binary Morphological Operations. – IET Computer Vision, Vol. **8**, 2014, No 6, pp. 718-728.

20. H a o, W., J. L i, X. Q u, Z. D o n g. Fast Iterative Contourlet Thresholding for Compressed Sensing MR. – Electronic Letters, Vol. **49**, 2013, No 19, pp. 1206-1208.

21. B h a t e j a, V., H. P a t e l, A. K r i s h n, A. S a h u. Multimodal Medical Image Sensor Fusion Framework Using Cascade of Wavelet and Contourlet Transform Domains. – IEEE Sensors Journal, Vol. **15**, 2015, No 12, pp. 6783-6790.

22. M a n s o u r, M., H. M o u h a d j e r, A. A l i p a c h a, K. D r a o u i. Comparative Analysis on Image Compression Techniques for Chromosome Images. – International Conference on Advances in Biomedical Engineering, 2013, pp. 34-37.

23. J e e n a, J., P. S a l i c e, J. N e e t h a. Denoising Using Soft Thresholding. – International Journal of Advanced Reseach in Electrical, Electronic and Instrumentation Engineering, Vol. **2**, 2013, No 3, pp. 1027-1032.

24. C h a n g, S. G., B. Y u, M. V a t t e r e l i. Adaptive Wavelet Thresholding for Image Denoising and Compression. – IEEE Transactions of Image Processing, Vol. **9**, 2000, No 9, pp. 1532-1546.

25. J a n s e n, M. Noise Reduction by Wavelet Thresholding. New York, Springer Verlag, Inc., 2001.

26. F o d o r, I. K., C. K a m a t h. Denoising through Wavelet Shrinkage: An Empirical Study. Center for Applied Science Computing Lawrence Livermore National Laboratory, 2001.
27. D o n o h o, D. L., J. M. J o h n s t o n e. Ideal Spatial Adaptation by Wavelet Shrinkage. – Biometrika, Vol. **81**, 1994, No 30, pp. 425-455.
28. D e n g w e n, Z., W. C h e n g. Image Denoising with an Optimal Threshold and Neighbouring Window. – Journal Pattern Recognition Letters, Vol. **29**, 2008, No 11, pp. 1603-1704.
29. D e w a n g a n, N., A. D. G o s w a m i. Image Denoising Using Wavletthresholding Methods. – Int. J. of Engg. Sci. & Mgmt. (IJESM), Vol. **2**, 2012, No 2, pp. 271-275.
30. K a l r a, G. S., S. S i n g h. Efficient Digital Image Denoising for Gray Scale Images. – Multimedia Tools and Applications, Vol. **75**, 2016, No 8, pp. 4467-4484.
31. H o s o t a n i, F., Y. I n u z u k a, M. H a s e g a w a, S. H i r o b a y a s h i, T. M i s a w a. Image Denoising with Edge-Preserving and Segmentation Based on Mask NHA. – IEEE Transactions on Image Processing, Vol. **24**, 2015, No 12, pp. 6025-6033.
32. D h a n n a w a t, R., A. B. P a t a n k a r. Improvement to Blind Image Denoising by Using Local Pixel Grouping with SVD. – Procedia Computer Science, Vol. **79**, 2016, pp. 314-320.
33. G u o, X., Y. L i, T. S u o, J. L i a n g. De-Noising of Digital Image Correlation Based on Stationary Wavelet Transform. – Optics and Lasers in Engineering, Vol. **90**, 2017, pp. 161-172.
34. C a n d e s, E. J., D. L. D o n o h o. Ridgelets: A Key to Higher-Dimensional Intermittency?. – Phil. Trans. R. Soc. Lond. A., Vol. **357**, 1999, No 1760, pp. 2495-2509.
35. C a n d è s, E., D. D o n o h o. Curvelets: A Surprisingly Effective Nonadaptive Representation for Objects with Edge. – In: A. Cohen, C. Rabut, L. Schumaker, Eds. Curves and Surface Fitting: Saint-Malo. Vanderbilt University Press, Nashville, 2000, pp. 105-120.
36. D o, M. N., M. V e t t e r l i. Thecontourlet Transform: An Efficient Directional Multiresolution Image Representation. – IEEE Trans. Image Process., Vol. **14**, 2009, No 12, p. 2091.
37. L e P e n n e c, E., S. M a l l a t. Sparse Geometric Image Representations With Bandelets. – IEEE Transactions on Image Processing, Vol. **14**, 2005, No 4, pp. 423-438.
38. P e y r é, G., S. P. M a l l a t. Surface Compression with Geometric Bandelets. ACM Transactions on Graphics. – Proceedings of ACM SIGGRAPH, Vol. **24**, 2005, No 3, pp. 601-608.
39. C h e n, G. Y.. T. D. B u i, A. K r z y z a k. Image Denoising with Neighbour Dependency and Customized Wavelet and Threshold. – Pattern Recognition, Vol. **38**, 2005, No 1, pp. 115-124. DOI:10.1016/j.patcog.2004.05.009.
40. Z h o u, D., W. C h e n g. Image Denoising with an Optimal Threshold and Neighbouring Window. – Elsevier Pattern Recognition, Vol. **29**, 2008, No 11, pp. 1694-1697. DOI: 10.1016/j.patrec.2008.04.014.
41. X i e, X. Research on the Image Denoising Method on Partial Differential Equations. – Cybernetics and Information Technologies, Vol. **16**, 2016, No 5, pp. 109-118.
42. H a s h i m o t o, F., H. O h b a, K. O t e, A. T e r a m o t o, H. T s u k a d a. Dynamic PET Image Denoising Using Deep Convolutional Neural Network without Prior Traning Datasets. – IEEE Access, Vol. **7**, 2019, No 5, pp. 96594-96603.
43. C h e n, W., Y. S h a o, L. J i a, Y. W a n g, Q. Z h a n g, Y. S h a n g, Y. L i u, Y. C h e n, Y. L i u, Z. G u i. Low-Dose CT Image Denoising Model Based on Sparse Representation by Stationarily Classified Sub-Dictionaries. – IEEE Access, Vol. **7**, 2019, No 5, pp. 116859-116874.